2021-1156 IJOI
https://www.ijoi-online.org/

COMPARISON OF REPAIR METHODS FOR CRACKED EARTH DAMS BASED ON DIFFERENT TECTONIC EARTHQUAKE EFFECTS

Tse-Shan Hsu
President, Institute of Mitigation for Earthquake Shear Banding Disasters
Professor, Department of Civil Engineering, Feng-Chia University, Taiwan R.O.C.
tshsu@fcu.edu.tw

Kuang-Chi Liao
Student, Ph.D. Program for Civil Engineering, Water Resources Engineering, and Infrastructure Planning, Feng-Chia University, Taiwan, R.O.C.

Zong-Lin Wu, Shey-En Chiu, Po-Liang Lin, Jia-De Lai
Directors, Institute of Mitigation for Earthquake Shear Banding Disasters, Taiwan R.O.C.

Yi-Min Huang
Assistant Professor, Feng-Chia University, Respectively, Taiwan, R.O.C.

Abstract

The Hutoupi Earth Dam is the first dam built in Taiwan. Since the dam was completed in 1863, it has suffered from cracks and piping failures from numerous tectonic earthquakes. After damage to the dam, the reservoir management agency immediately repaired it. However, as the seismic design only fortified the dam against the secondary ground vibration effect of tectonic earthquakes and ignored the primary shear banding effect, the problem of cracking or piping failure continued to occur after the repairs were completed. Therefore, in this study, two different cracking mechanisms are proposed for earth dams: ground vibrations and shear banding.

The performance of the repair methods is then compared based on these two cracking mechanisms. Three findings are drawn from the results. (1) When the engineering design for the repair is based on the ground vibration cracking mechanism, only a limited crack extension and depth can be repaired; therefore, the shear bands and shear textures in the deeper sections of the earth dam are ignored, causing cracking problems that cannot be resolved completely. (2) When the engineering design of the repair is based on the shear band extension mechanism, an appropriate extension range and depth for the shear bands can be selected after weighing safety and costs. Designing for these ranges can effectively suppress the occurrence of cracks. (3) Restoration projects must choose backfill materials that have low permeability and are resistant to shear banding and ground vibration. By implementing comprehensive quality management methods, the compacted soil can perform according to its functional needs. Based on these three findings, it is recommended that the shear banding effect be included in the seismic design code for earth dams to prevent cracks and piping failure in the earth dams and thus perform according to the design goals.

Keywords: tectonic earthquakes, shear banding, ground vibrations, cracking, piping failure.

Introduction

Taiwan, which is located on the edge of the Eurasian Continental plate, experiences frequent tectonic earthquakes from the compression of the Philippine Sea Plate. Prototypes of various structures are often subjected to tectonic earthquake tests. Between 1863, when the Hutoupi Earth Dam in Taiwan was completed, and 2000, several tectonic earthquakes caused cracks or piping failures at the turning area (Jianan Farmland Water Conservancy Association, 2012) shown in Figure 1.

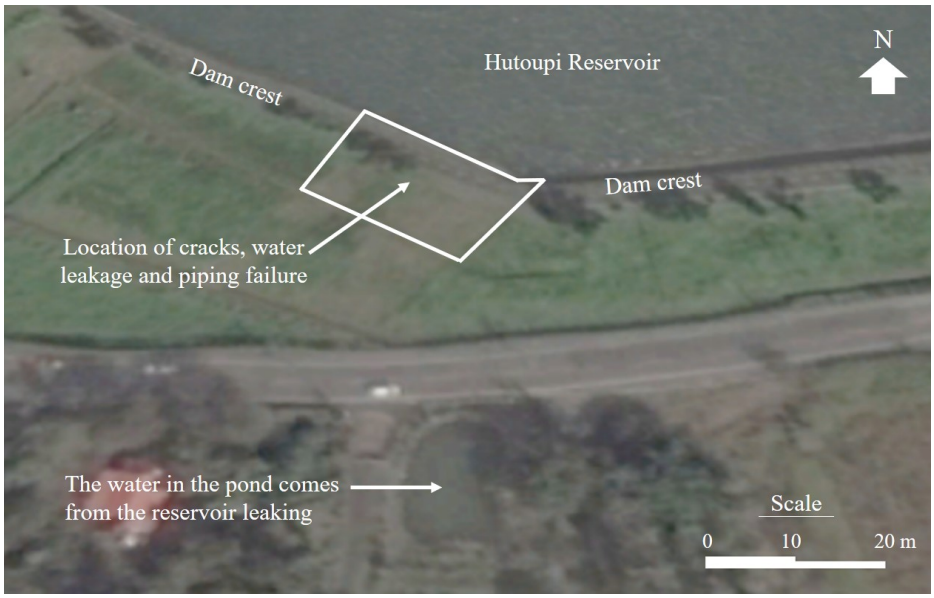

Figure 1. The location of the Hutoupi Earth Dam, in which cracks, water leakage, and piping failure have repeatedly occurred (the background picture is from Google Earth, 2021).

While the current literature reporting on the piping failure at the Hutoupi Earth Dam (Jianan Farmland Water Conservancy Association, 2012) is limited to textual descriptions, piping failure at the turn of the study site shown in Figure 1 is similar to the piping failure at a different site as shown in Figure 2. Therefore, it is very important to study the mechanism that drives the piping failure (Terzaghi and Peck, 1967) at the turn of the earth dam and to investigate effective repair methods.

Figure 2. Example of piping failure at the turn of an earth dam (Wendy Fisher, 2021).

Cracking Mechanism of Earth Dams During a Tectonic Earthquake

Generally, there are five types of earthquakes: tectonic, volcanic, subsidence, earthquakes induced by reservoir storage, and earthquakes induced by artificial explosions (China Earthquake Disaster Prevention Center, 2021). In tectonic earthquakes, the most common type, the main effect is shear banding, which accounts for more than 90% of the total energy of the earthquake. A secondary effect of tectonic earthquakes is ground vibrations, which only account for less than 10% of the total energy of tectonic earthquakes (Coffey, 2021; Hsu, et al., 2017).

In terms of displaced terrain features, river valleys and river banks are derived from the shear-band tilting effect, so the turn of the earth dam is the necking area after the intersection of rivers with different orientations, and therefore the shear bands existing in the valley and river bank at the turn of the earth dam will extend into the earth dam during tectonic earthquakes (see Figure 3a), and when the upstream reservoir water table rises, the brittle fracture of the shear bands will cause water leakage if the degree of brittle fracture is light (see Figure 3b to Figure 3d), and if it is severe, it will cause piping failure (see Figure 4).

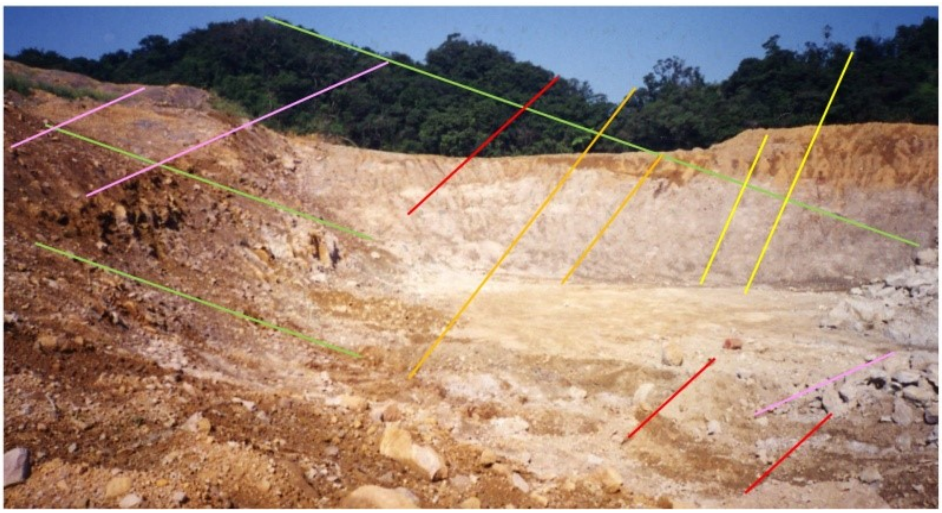

(a) After the earth dam was excavated, it was discovered that the shear bands from the valley and river bank had extended into the earth dam.

(b) The location of the leak in the earth dam (Google Earth, 2021; Data from Lin, 2009).

(c) On-site water leakage phenomenon 1.

(d) On-site water leakage phenomenon 2.

Figure 3. Water leakage induced by the extension of shear bands into the earth dam (Xinshan Earth Dam, Taiwan; Lin, 2009).

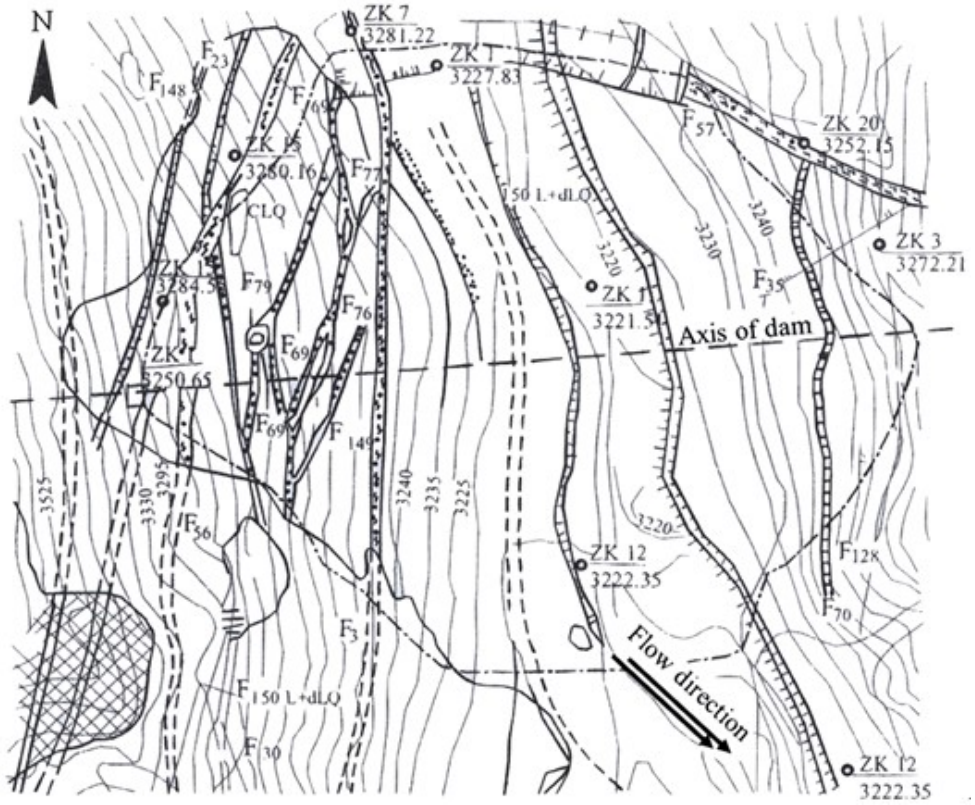

(a) Plan view of the shear bands in the river valley and river bank.

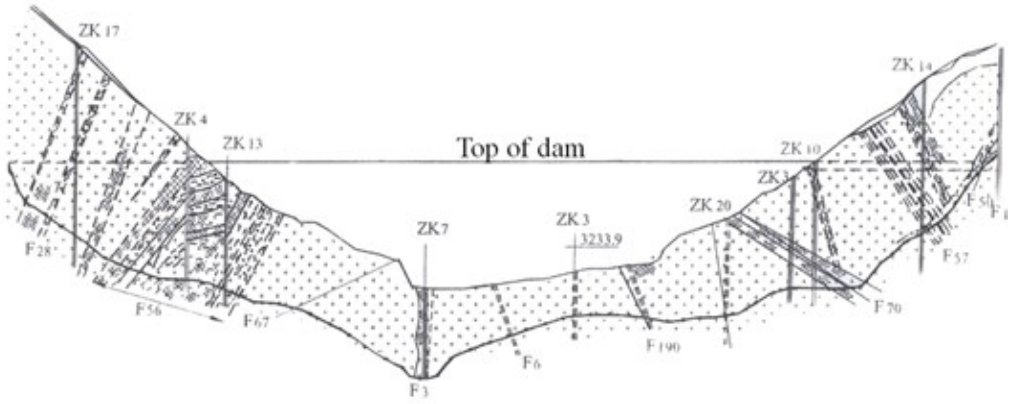

(b) Sectional view of shear bands in the river valley and river bank.

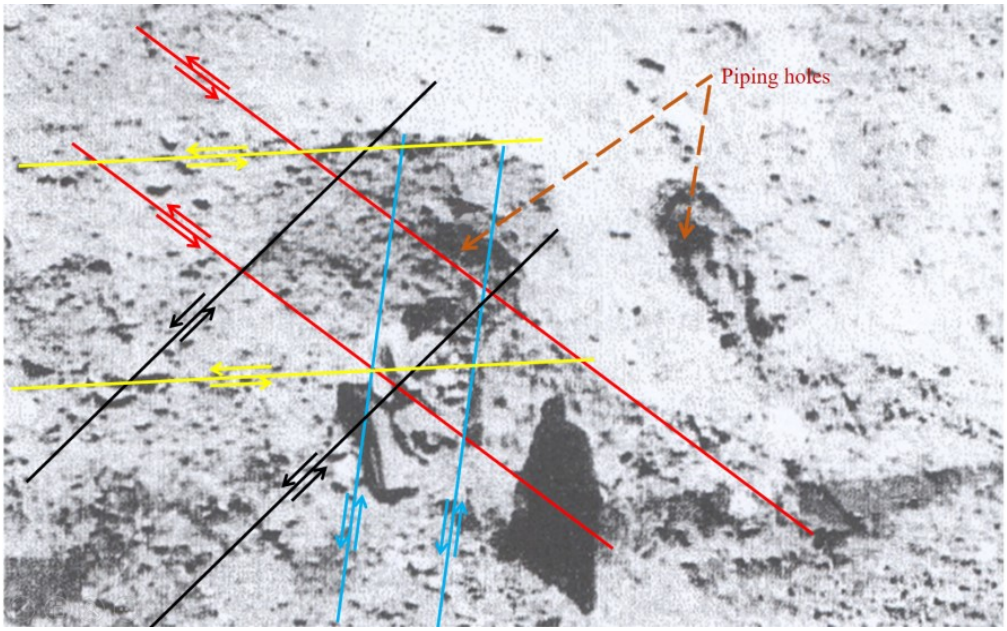

(c) The piping holes induced by the shear bands extending into the earth dam.

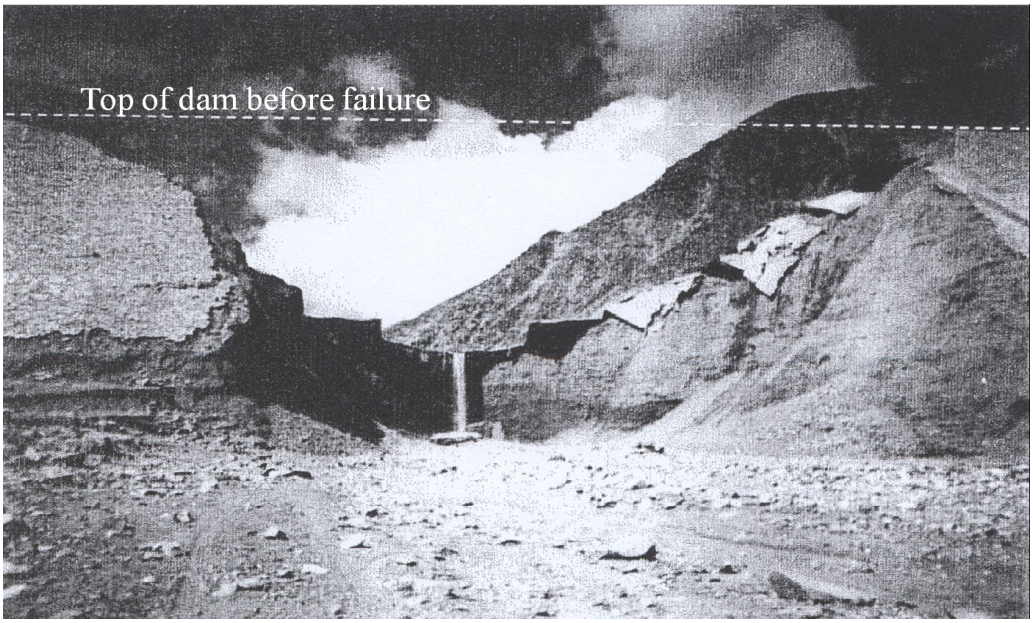

(d) The piping failure induced by the shear bands extending into the earth dam.

Figure 4. Views of shear bands that extend into an earth dam and some examples of the resulting damage (Sinotech Foundation for Research and Development of Engineering Sciences and Technologies, 2008).

Although ground vibrations are a secondary effect of tectonic earthquakes, traditional scholars and technicians still believe that ground vibrations are the main cause of cracks in earth dams. Therefore, the seismic design code (Geotechnical Engineering Manual, 2015; Natural Resources Conservation Service Construction Specifiction, 2021; Stephens, 2010; US Army Corps of Engineers, 2004; US Department of the Interior, Bureau of Reclamation, 2012; Water Resources Agency, MOEA, 2003; Water Resources Agency, MOEA, 2008) only fortify the dam against ground vibrations. Furthermore, as the acceleration increases with increased dam elevation during the ground vibrations, cracks in the earth dam from ground vibrations are believed to only appear locally on the top of the dam and on the surface of the downstream slope near the top of the dam (see Figure 5).

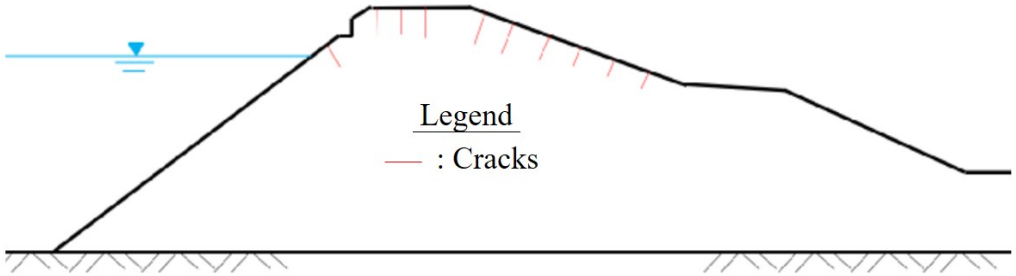

Figure 5. The mechanism for earth dam cracking inducement by ground vibrations (redrawn from Jianan Farmland Water Conservancy Association, 2012).

The mechanism for the extension of shear bands into the earth dam

During tectonic earthquakes, shear bands in the valley and river bank extend into the earth dam, which is the main source of cracking in earth dams. Therefore, when the seismic design code only fortifies the dam against ground vibration, it is impossible to prevent the occurrence of earth dam cracking caused by shear banding. Thus, a mechanism is proposed that could explain how the shear bands in the river valley and river bank extend into the earth dam (see Figure 6).

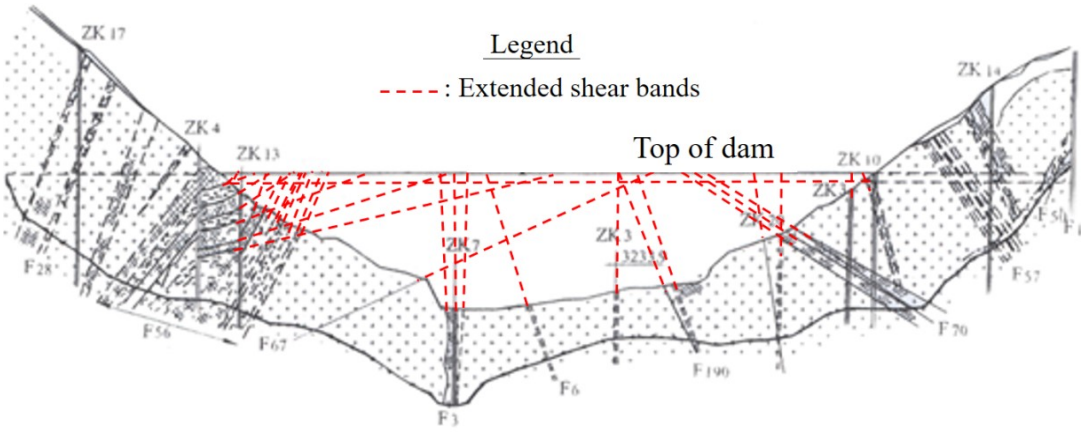

Figure 6. The mechanism for the extension of shear bands into the earth dam (the base map is from Sinotech Foundation for Research and Development of Engineering Sciences and Technologies, 2008).

Case Study

The Hutoupi Earth Dam, shown in Figure 1, is a homogeneous dam that cracked during the 2010 Jiaxian earthquake and the 2016 Meinong earthquake. After both cracking events, the damaged areas were repaired. As both tectonic earthquakes had a magnitude of 6.4, and since the repairs involved different restoration methods, the effectiveness of these different restoration methods can be compared through a case study.

Repair case study based on the ground vibration mechanism for earth dam cracking

After the turning point of the Hutoupi Earth Dam (see Figure 1) was cracked in the 2010 Jiaxian earthquake, the reservoir management agency immediately commissioned scholars and technicians to repair it according to conventional methods. Typically, traditional scholars and technicians perform design for the repair based on the ground vibration mechanism for earth dam cracking. Therefore, ground penetration radar and in-situ excavation methods were used to investigate the crack coverage and depth before the design (see Figure 7).

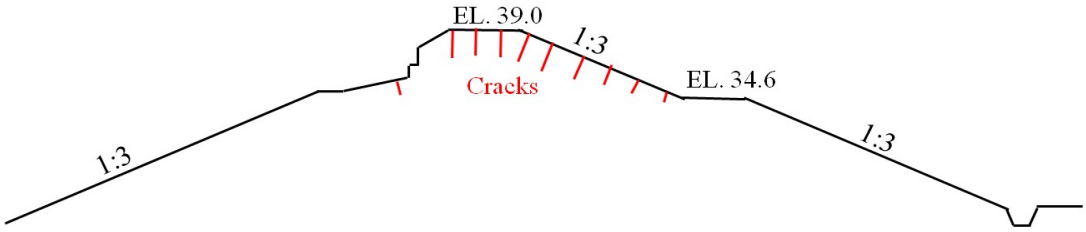

(a) The results of the survey using ground penetrating radar.

(b) The results of the investigation using in-situ excavation methods.

Figure 7. The coverage and depth of cracks as determined by conventional investigation methods (Jianan Farmland Water Conservancy Association, 2012).

Using the results of the investigation of the cracks, the engineering design for the repair was performed. Then, the site was excavated, layered with backfill, and rolled (see Figure 8). The backfill material was a mixture of the original dam body material and borrowed soil, which has properties that are nearly equal to those of the original earth dam material. The original earth dam material is classified as low-plasticity silt (ML) with a plasticity index (PI) of only 3.6; therefore, it does not meet the U.S. Bureau of Reclamation Design Code for homogeneous dams, which requires $7 \leqq PI \leqq 25$.

Figure 8. Layered backfilling and rolling operations for the Jiaxian Earthquake Restoration Project of the Hutoupi Earth Dam (Jianan Farmland Water Conservancy Association, 2012).

The Jiaxian Earthquake Restoration Project for the Hutoupi Earth Dam was completed in 2010. The condition of the earth dam's turn on February 14, 2013 (Figure 9a) was approximately the same as that of the completed project in 2010. However, a satellite image from November 23, 2013 shows that

the repaired earth dam began leaking again (see Figure 9b). Therefore, it can be concluded that the Jiaxian Earthquake Restoration Project, which was planned based on ground vibrations as the earth dam cracking mechanism, did not meet the requirements for withstanding shear banding during tectonic earthquakes, regardless of the material, coverage, or extension depth.

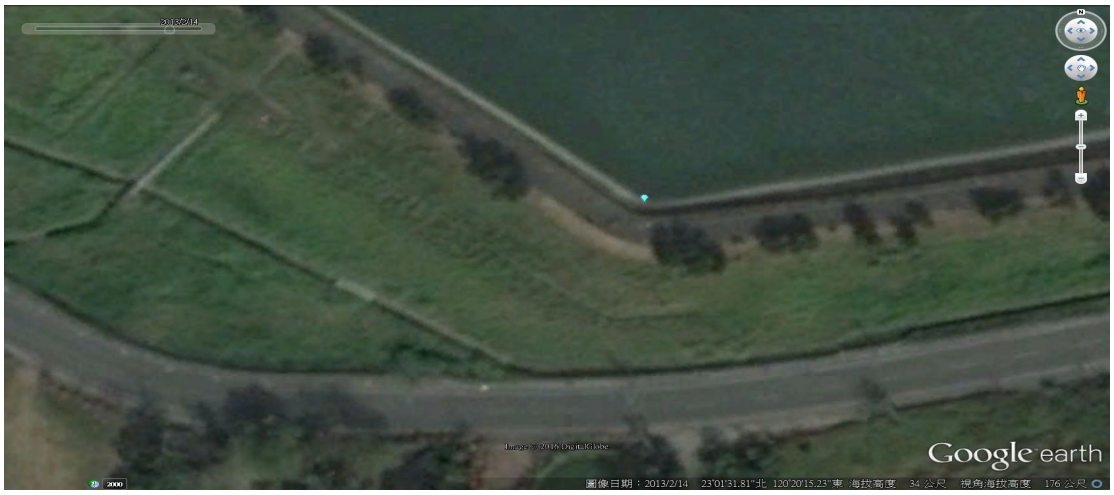

(a) February 14, 2013.

(b) November 23, 2013.

Figure 9. After the Jiaxian earthquake, the Hutoupi Earth Dam restoration project was completed, and the turning point leaked again (Google Earth, 2021).

A repair method based on shear band extension into the earth dam

1) Determination of repair range

The turning point of the Hutoupi Earth Dam (Figure 1) suffered a more serious cracking problem during the 2016 Meinong earthquake (Figure 10). Subsequently, the reservoir management agency commissioned the authors' group to identify the shear bands and to investigate the extension of the shear bands and shear textures in the Hutoupi Earth Dam.

(a) 2010 Jiaxian Earthquake.

(b) 2016 Meinong earthquake.

Figure 10. Comparison of the degree of cracking in the turn of the Hutoupi Earth Dam.

First, a GPS velocity vector distribution map was used for the area surrounding the Hutoupi Earth Dam turn (shown in Figure 11a), supplemented by the definition of shear bands (Hsu, 1987), to identify some of the shear bands in the Hutoupi Earth Dam turn (Figure 11b). The strike of the slip-type shear band (white line) is N51.7°W, the strike of the conjugate slip-type shear band (purple line) is N38.3°E, the strike of the twinning-type shear band (yellow line) is N0.2°E, and the strike of the conjugate twining-type shear band (orange line) is 89.8°W.

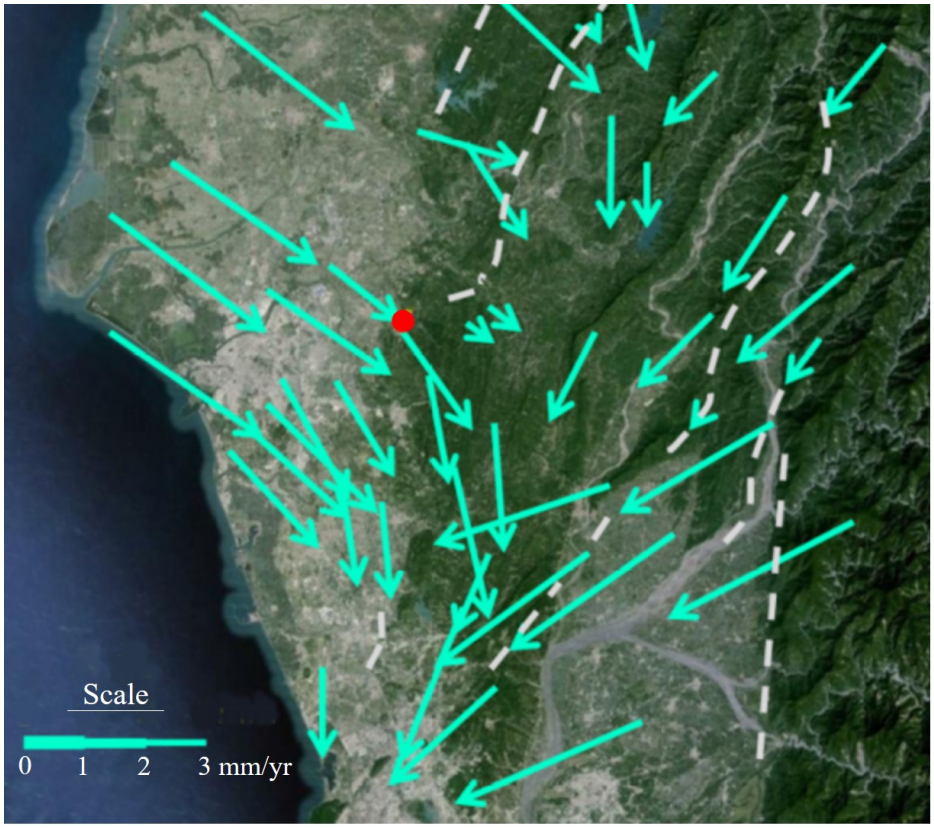

(a) GPS velocity vector distribution map.

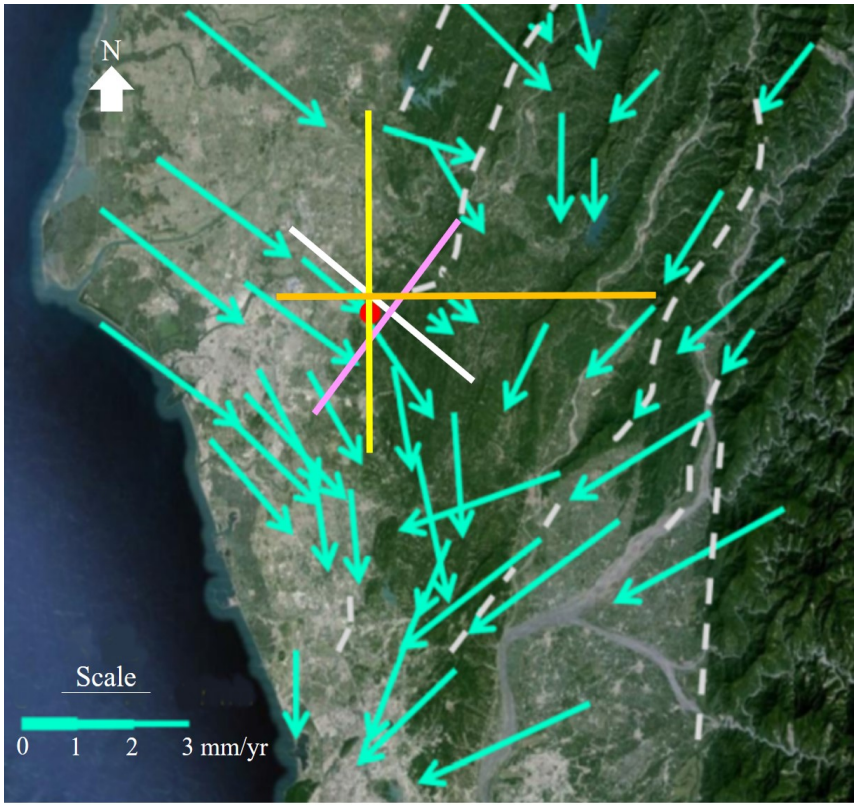

(b) Identified shear bands.

Note: The center of the red circle represents the turning point of the Hutoupi Earth Dam.

Figure 11. The shear bands at the turn of Hutoupi Earth Dam were identified using a GPS velocity vector distribution map (Google Earth, 2021; GPS LAB, 2007).

When the four groups of shear bands shown in Figure 11b in the valley and river bank dislocate, the shear textures of a shear band extend into the earth dam (Figure 12).

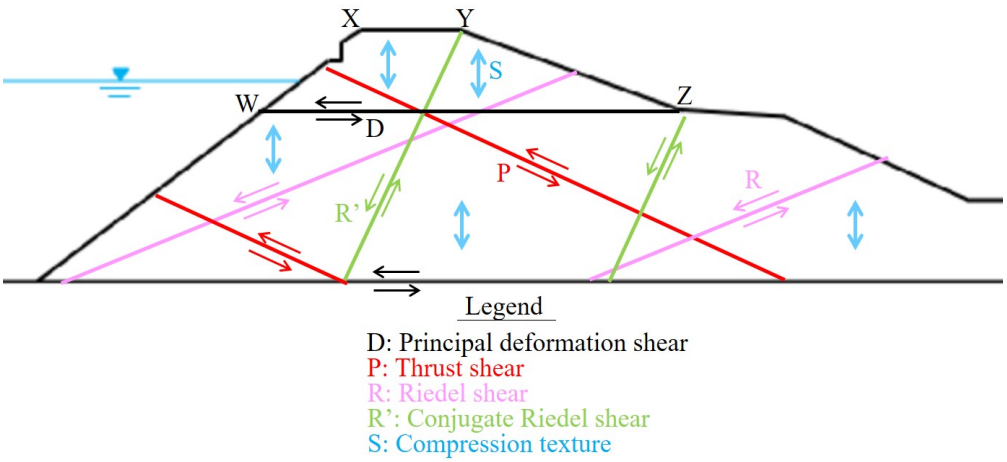

Figure 12. A schematic diagram of the shear textures of a shear band extending into the Hutoupi Earth Dam.

The excavated Hutoupi Earth Dam turn is shown in Figure 13a. Figure 13b shows that all five groups of shear textures, including the principal deformation shear D, thrust shear P, Riedel shear R, conjugate Riedel shear R', and compression shear (shown in Figure 12) extended into the turn of the Hutoupi Earth Dam.

(a) The east side of the turn with no shear textures overdrawn.

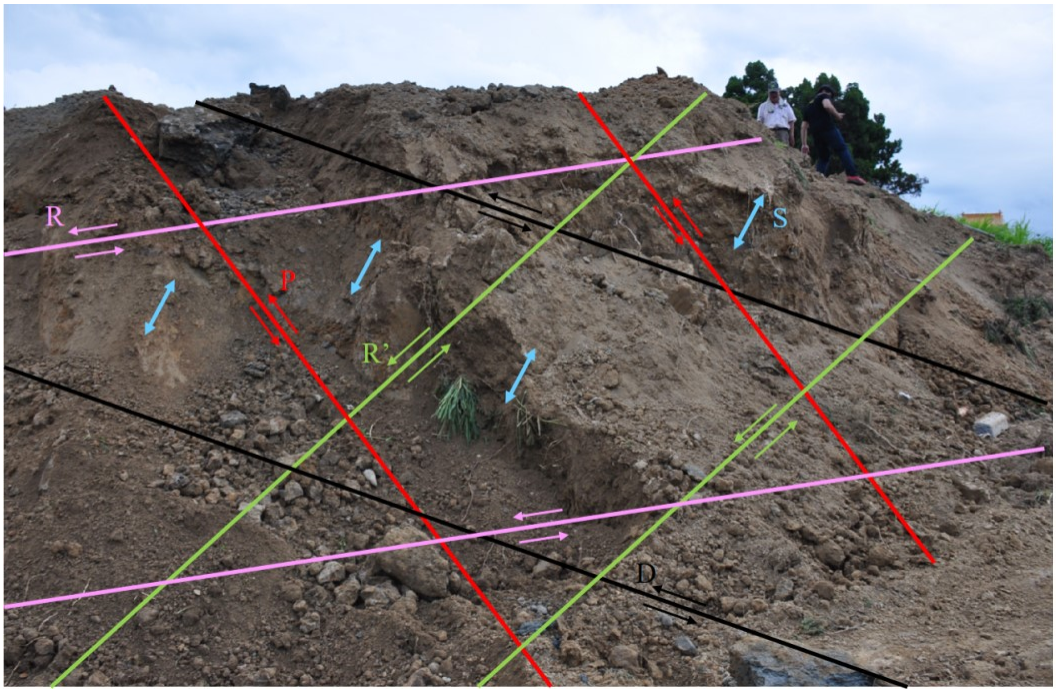

(b) After overdrawing the shear textures on the east side of the turn

(c) The west side of the turn with no shear textures overdrawn.

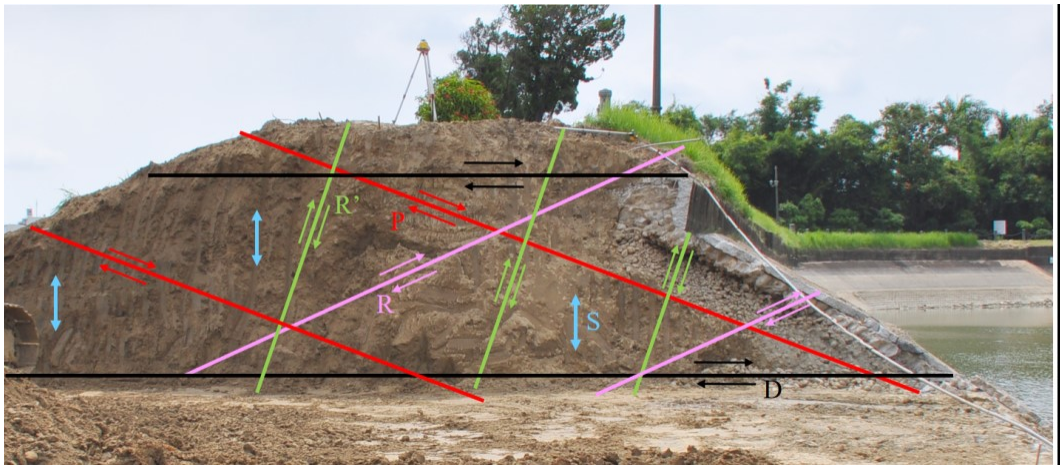

(d) The west side of the turn with overdrawn shear textures.

Figure 13. After the Meinong earthquake, the excavation of the Hutoupi Earth Dam revealed that the shear textures of a shear band extended into the earth dam.

Secondly, a field density test was conducted at the turning point of the Hutoupi Earth Dam shown in Figure 13. The results show that the repair project after the Jiaxian earthquake used low-plasticity silt (ML), and that after the shear textures extended into the earth dam, the relative compaction (RC) of the top of the earth dam was reduced from 98% at the time of completion to 84.9%; i.e., the void ratio *e* increased from 0.48 to 0.71. In this case, the pore spaces at the turn of the Hutoupi Earth Dam connected in series to form a tubular outlet, and under the influence of the following four factors, the reservoir water could easily flow out along the tubular outlet below the highest reservoir water table (Figures 2, 3b, and 9b).

(1) The cross section area closer to the crest of the embankment dam becomes smaller;
(2) The vertical confining pressure decreases closer to the crest of the dam;
(3) During tectonic earthquakes, the areas in the dam body closer to the embankment dam crest experience greater vibration accelerations;
(4) During tectonic earthquakes, the areas in the dam body closer to the crest of the dam experience greater brittle fracture in the soil from shear banding.

Based on the results of the investigation, the longitudinal repair range of

the Hutoupi Earth Dam turn was chosen as shown in Figure 14. The cross-sectional repair range is shown in Figure 12 as the $\overline{WXYZ}$ range.

Figure 14. Longitudinal repair range for the Hutoupi Earth Dam turn.

2) Selection of backfill material

Homogeneous earth dams must be able to simultaneously withstand the effects of shear banding and ground vibrations during tectonic earthquakes. The original earth dam material was low plasticity silt (ML), which has very low resistantance to shear banding. Therefore, for the restoration project after the Meinong earthquake, clayey gravel (GC) was used, which has low permeability and high resistance to shear banding (Wagner, 1957). The composition of GC is 34.77% fine-grained materials such as silt and clay, 30.23% sand, and 35% gravel. Since the PI of fine-grained materials is 11.3, it meets the requirements of the US Bureau of Reclamation Design Code for homogeneous dams, which requires 7□PI□25 (US Department of the Interior, Bureau of Reclamation, 2012).

3) Determination of the maximum dry unit weight and optimal moisture content for the overall soil

Since the gravel content of the material was greater than 30%, a large-scale compaction test must be conducted, or the correction formula proposed by Hsu and Saxena (1991) must be used to correct the influence of the over-sized particles on the maximum dry unit weight of the whole soil.

Since large-scale compaction tests are very time-consuming, they are not suitable for emergency repair projects, such as the repair of an earth dam. Therefore, after completing the standard Proctor compaction test, Equation 1, which was proposed by Hsu and Saxena (1991), was used to modify the maximum dry unit weight $\gamma_{d,\max}$ of the compacted soil with a gravel content P of 0% to determine the maximum $\gamma_{dT,\max}$ for the overall soil with a gravel content P of 35%. The unit weight of the dry soil and Equation 2 can be used to modify the optimum moisture content (OMC) of the compacted soil for a gravel content P of 0% to find the optimum moisture content (OMC_T) of the overall soil for a gravel content P of 35%.

$$\gamma_{T,\max} = \frac{1}{(1+e_T)\cdot\left(\frac{P}{G_g\gamma_w}+\frac{1-P}{G_s\gamma_w}\right)}. \quad \text{(Equation 1)}$$

$$OMC_T = OMC\cdot(1-P). \quad \text{(Equation 2)}$$

In Equation 1, G_g is the specific gravity of the gravel remaining on a No. 4 U.S. standard sieve, with a value of 2.640, G_s is the specific gravity of the soil that passed through the U.S. standard sieve, with a value of 2.672, and e_T is the void ratio of the overall soil, which can be calculated using Equation 3.

$$e_T = e + AP + BP^2 + CP^3 + DP^4. \quad \text{(Equation 3)}$$

In Equation 3, e is the void ratio corresponding to the maximum dry unit weight of the compacted soil with P = 0%, A = -0.442861167, B = -0.088452600, C = 0.979631467, and D = -0.519465600 (Hsu and Saxena, 1991).

For compacted soil with a gravel content of P is 0%, $\gamma_{d,\max}$ is 18.123kN/m^3, OMC is 14.3%, and the corresponding void ratio e is 0.4459 according to the standard Proctor compaction test. For the overall compacted soil with a gravel content P of 35%, the void ratio (e_T = 0.314) can be calculated using Equation 3, the dry unit weight ($\gamma_{dT,\max}$ = 19.849kN/m^3) can be calculated using Equation 1, and the optimal water content (OMC_T = 9.3%) can be calculated using Equation 2.

4) A comprehensive quality management method for compacted soil

After the excavation of the restoration project area was completed, samples of gravel, sand, and fine-grained soils were collected from the borrowing area. Using a maximum gravel particle size of 7.62 cm and allowed permissible thickness for each layer of soil after rolling of 30 cm, the total dry weight $W_{d,n}$ required for the n^{th} layer was calculated from the volume of the n^{th} layer of the restoration area and the maximum dry unit weight ($\gamma_{dT,\max}$ = 19.849kN/m^3) of the overall soil. Then, the dry weight of the gravel, sand, and fine-grained soil composed of various particle sizes was calculated according to the particle size distribution curve, and water was added to yield to an OMC_T of 9.3%. Finally, after uniform mixing, the soil was transported to the restoration area and was evenly distributed.

To effectively ram the GC, a rolling machine with a mass of 10 Mg (shown in Figure 15) was rolled back and forth until all the control points in the n^{th} layer surface reached an elevation that corresponded to $\gamma_{T,\max}$ = 19.849kN/m^3.

Figure 15. Rehabilitation of the turn of the Hutoupi Earth Dam after the Meinong earthquake.

A large-scale field density test with dimensions of 50 cm length x 50 cm width x 30 cm height was completed for the compacted soil under total quality management. The relative compaction (RC) according to the test reached 100% (the contract required a value greater than 98%). The test results also demonstrated that the water content was between OMC_T and $OMC_T + 1\%$; i.e., the compaction quality of the overall clayey gravel met the requirements of the construction code.

5) Repair effectiveness

Figure 16 shows the status of the restoration work at the turn of the Hutoupi Earth Dam after its completion in August 2016.

Figure 16. The turning point of the Hutoupi Earth Dam after completion of the restoration project (August 2016).

Since the completion of the restoration project after the Meinong earthquake, seventy-one tectonic earthquakes with M_L = 5.0 to 5.4, twenty-nine tectonic earthquakes with M_L = 5.5 to 5.9, and twelve tectonic earthquakes with M_L = 6.0 to 6.7 have occurred in Taiwan. However, the turning area of the Hutoupi Earth Dam has not experienced cracking problems during this time.

Discussion And Comparison Of Results

Comparison of slope stability safety factors after completion of different restoration projects after tectonic earthquakes

First, a slope stability analysis was performed upon completion of the restoration project after the Jiaxian earthquake in 2010. The analysis profile contained three soil layers: the restored soil layer after the Jiaxian earthquake, the soil layer of the original earth dam, and the soil layer under the dam. Since these three soil layers have similar properties and are classified as low plastic silt (ML), their properties were considered to be equal, with a unit weight of 17kN/m^3, a cohesive force of 5.0kN/m^2, and a friction angle of 26^o. The quasi-static horizontal seismic acceleration coefficient k_h of 0.15 and the vertical seismic acceleration coefficient k_v of 0.075 were converted from the

peak ground acceleration in the tectonic earthquake.

The results of the slope stability analysis based on this data are shown in Figure 17. For the ground vibration conditions, Figure 17 shows the sliding surfaces that correspond to five smallest slope stability safety factor after the Jiaxian earthquake. The slope stability safety factor for the sliding surface marked with * is the minimum value of 0.998.

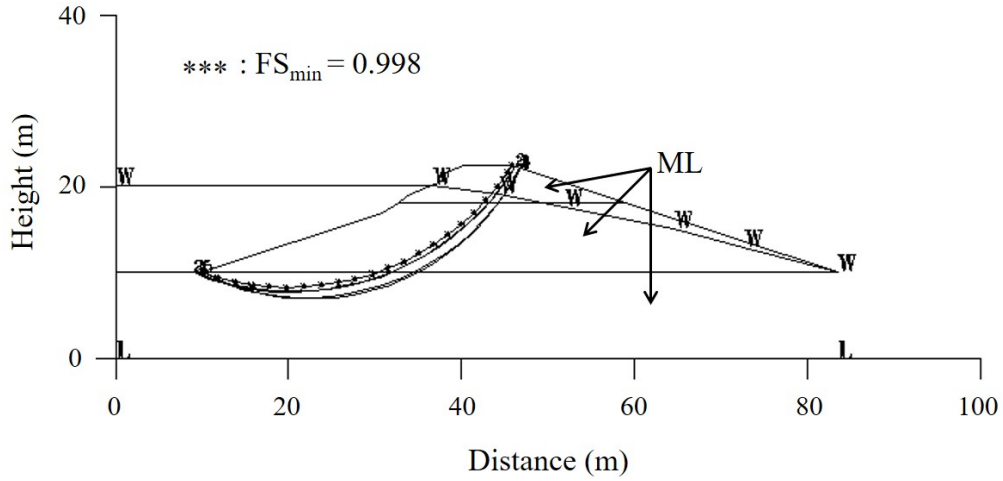

Figure 17. The slope stability analysis results for the restoration project using vibration records from the Jiaxian earthquake.

Second, a slope stability analysis was performed upon completion of the restoration project after the Meinong earthquake in 2016. The analysis profile contained three soil layers: the restored soil layer after the Meinong earthquake, the soil layer of the original earth dam, and the soil layer under the dam. The properties of the restored soil layer after the Meinong earthquake differ from those of the original earth dam and the soil layer below the dam. However, the properties of the soil layer of the original earth dam and the soil layer below the dam are equal to those described above. Since the repaired soil layer after the Meinong earthquake is GC, its properties include a soil unit weight of 19.849kN/m^3, a cohesive force of 70kN/m^2, and an internal friction angle of 36^o. The quasi-static horizontal and vertical seismic acceleration coefficients used in the analysis are also the same as those listed above.

The results of the slope stability

analysis using these results are shown in Figure 18. For the ground vibration conditions, Figure 18 shows the sliding surfaces that correspond to the five smallest slope stability safety factors after the Meinong earthquake. The slope stability safety factor for the sliding surface marked with * is the minimum value of 1.309.

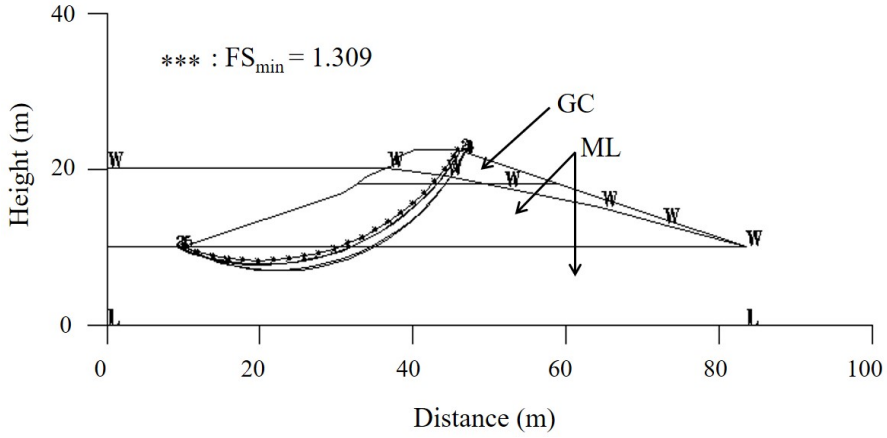

Figure 18. The slope stability analysis results of the restoration project using vibration records from the Meinong earthquake.

The restoration project after the Jiaxian earthquake incorporated low plastic silt, which has a very low shear banding resistance, so the shear bands and textures from the original valley or river bank could easily enter the earth dam. Therefore, after the earth dam experienced local brittle fracture, the void ratio in the fractured zone increased significantly. Once the material of the earth dam softens, the slope stability safety factor during ground vibrations becomes less than 0.998 (the value obtained from the analysis), so the structure is prone to local collapse, as shown in Figure 14.

By contrast, the restoration project after the Meinong earthquake incorporated GC with a high resistance to shear banding, so the shear textures from the original valley or river bank could not easily enter the earth dam. The earth dam has a high shear resistance strength and can ensure that the slope stability safety factor is greater than 1.2 during ground vibrations. Therefore, although there have been seventy-one tectonic earthquakes with M_L = 5.0 to 5.4, twenty-nine tectonic earthquakes

with M_L = 5.5 to 5.9, and twelve tectonic earthquakes with M_L = 6.0 to 6.7, no cracks have appeared at the turn of the earth dam after the repair.

Comparison of groundwater seepage and pipe flow in earth dams

Earth dams can be divided into non-shear banding zones and shear banding zones. When reservoir water flows through the non-shear banding zone of the earth dam, its flow pattern follows the steady-state seepage behavior described in conventional soil mechanics. During seepage, the soil mass is conserved, so soil will not flow out with the groundwater. However, when reservoir water flows through the shear banding zone of the earth dam, its flow pattern does not follow the steady-state seepage flow described in conventional soil mechanics, but rather unsteady pipe flow. In pipe flow, soil mass is not conserved, so soil will flow out with the groundwater.

Figure 1 shows a pond of water located approximately 50m south of the turn of the Hutoupi Earth Dam. It is observed that the soil fines entrained by reservoir water flowing downstream along the shear bands or textures that extended into the earth dam (see Figure 11b). Since soil mass was not conserved during flow into the pond, this groundwater flow pattern is an unsteady pipe flow.

Since the average slope between the Hutoupi Reservoir and the pond is approximately 6.8^{o}, the soil fines that may accompany the flow of groundwater have a particle size between 0.002 mm and 0.075 mm, a specific gravity G_S of 2.69, and a void ratio e of 0.71. Therefore, according to Equation 4, the critical bottom velocity of the soil fines required for the groundwater to flow through the shear bands or textures with floating soil fines is between 0.62cm/s and 3.76cm/s. The critical bottom velocity of soil fines is much greater than the seepage velocity of groundwater in low-plasticity soil fines (< 10^{-5}cm/s) when the hydraulic gradient is 1.0; therefore, it can be shown that the water flow pattern through shear bands or shear textures, follows unsteady state pipe flow, not steady state seepage flow.

$$v_{bc} = \sqrt{\frac{2g(G_s - 1)}{1 + e}} \cdot \sqrt{D} \cdot \cos\beta \,. \qquad \text{(Equation 4)}$$

Comparison of cracking mechanisms in earth dams during tectonic earthquakes

Procedure 1 in Figure 19 shows a tectonic plate subjected to lateral compression. When the strain enters deep into the plastic range and the material undergoes strain softening, the plate loses the ellipticity required for structural stability, and localizations of deformations occur, which in turn results in the formation of shear bands (Hsu, 1987; Rice, 1976; Rudnicki and Rice, 1975; Valanis, 1989). Procedure 2a in Figure 19 shows that highly concentrated pore water pressures appear in the shear bands. Procedure 2b in Figure 19 shows the relationship between the friction resistance formed during shear banding and the stick-slip phenomenon continues to appear. Procedure 3 in Figure 19 shows that when a stick (green arrow in Figure 19) occurs, the tectonic plate appears to decelerate, and when a slip (red line in Figure 19) occurs, the tectonic plate appears to accelerate. As a result, the deceleration-acceleration phenomenon repeats on the acceleration-time curve.

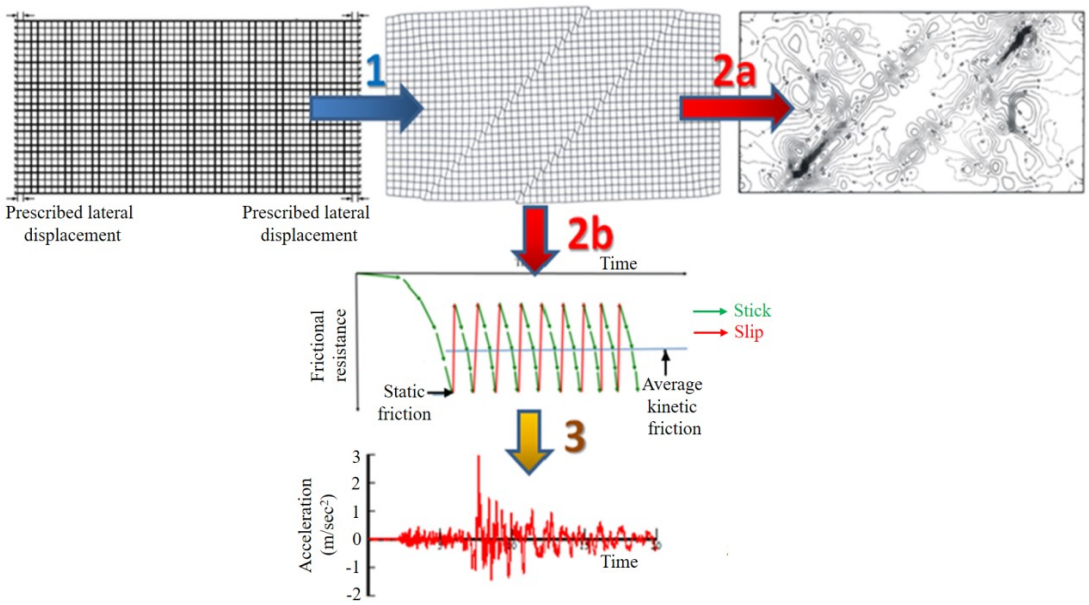

Figure 19. The mechanism in which ground vibrations are induced by the shear banding in tectonic earthquakes (Hsu, 2018).

Therefore, the main effect of tectonic earthquakes is shear banding, which appears locally, while the secondary effect is ground vibrations,

which can be felt throughout the tectonic plate and are induced by shear banding.

As the cracking phenomenon in the Hutoupi Earth Dam did not appear everywhere, the three constituent elements of the major cause for disasters proposed by Hsu, Hsieh and Lai (2009) could be applied (uniqueness, integrity, and comprehensiveness) to examine the ground vibrations that occur in all tectonic earthquakes. The ground vibrations in the Hutoupi Earth Dam turn was not attributable to the major cause. Therefore, the major cause for the local cracking phenomenon in the Hutoupi Earth Dam turn is the local slip and twinning shear bands that extend from the river bed and the river bank into the turn of the earth dam during tectonic earthquakes (detailed in Figure 11).

Thus, considering the earth dam cracking mechanism as being based only on ground vibrations addresses only the secondary effects of tectonic earthquakes. When the cracks extend from the top of the dam downwards, only a very limited extension depth can be detected. Therefore, the design of the restoration project does not meet the actual requirements of the dam, so cracks, water leakage, or piping damage may easily occur after the completion of the repair project.

Since the shear banding mechanism meets the requirements of the main effects of tectonic earthquakes, when shear bands or shear textures extend from the valley or river bank into the turn of the earth dam, cracks occur on the crest of the dam in the shear banding zone. Observations have shown that the shear bands and shear textures extended to the top of the dam; therefore, the safest design for the repair project should consider the full section at the turn of the earth dam. However, as the restoration project design must consider both the safety of the earth dam and the minimum water table of the reservoir, the design result for the restoration project was limited to the $\overline{\text{WXYZ}}$ section shown in Figure 12. The impact of the soil fines entrained by reservoir water flowing downstream along the shear bands or shear textures in the soil layers below the $\overline{\text{WXYZ}}$ section (shown in the pond in Figure 1) on the safety of the earth dam can be evaluated through the results of a slope stability analysis performed before construction.

Therefore, for the Hutoupi Earth Dam turn, only a restoration project design that considers the shear banding mechanism can safely and effectively reduce the influence of shear banding and ground vibrations in tectonic earthquakes.

Comparison of conventional quality management and total quality management approaches for compacted soils

As construction sites for compacted soil in Taiwan use the conventional quality management approach, no ovens have been equipped, so it is difficult to accurately determine the wet weight, water content, and dry weight of the borrowed soil. Therefore, the amount of water added to the overall soil cannot be accurately calculated, and a field survey has not been performed during the layered compaction process. This results in an uneven distribution of moisture content and the field dry density of the compacted soil.

To address the shortcomings of conventional quality management and to uniformly distribute the moisture content and the field density of the compacted soil, a total quality management approach was adopted for the first time for the restoration of the Hutoupi Earth Dam's turn after the Meinong earthquake, so that the entire area of the restoration project met the construction specifications. The following workflow chart describes the execution procedure:

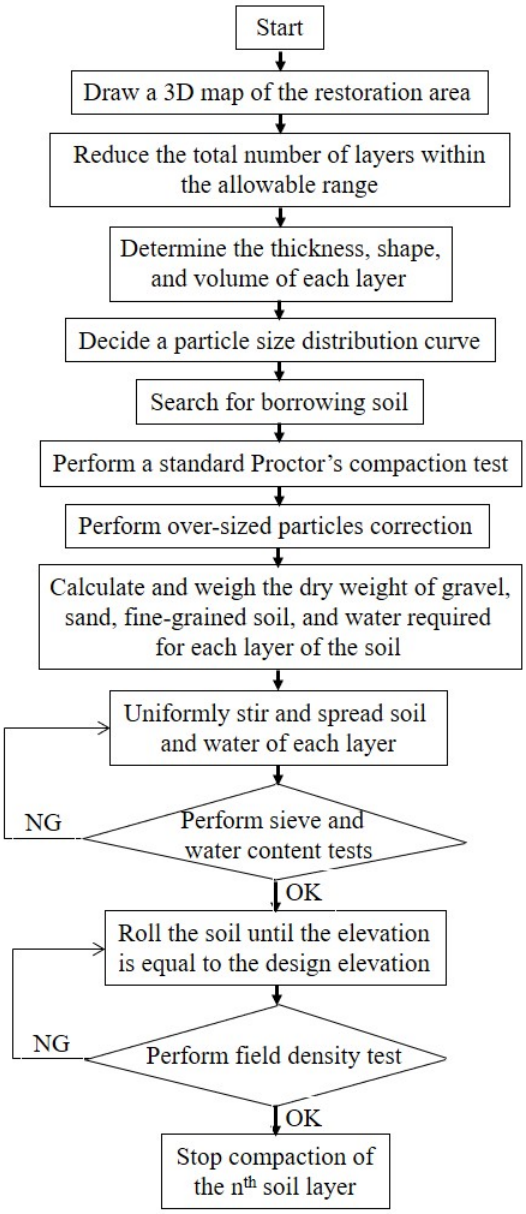

Figure 20. Workflow chart of comprehensive quality management for compacted soil of restoration area.

When the soil meets the field density and water content contractual obligations, its properties will become stable and will not be affected by rain; therefore, before spreading each layer of soil, the weather report must be consulted to ensure that it will not rain during the rolling operation after spreading.

Conclusions and Suggestions

Generally, earth dam cracking precedes piping failure. Earth dam piping failures can cause a large number of deaths and property losses. Therefore, it is invaluable to share effective earth dam repair engineering design methods.

This study compared the effectiveness of different repair methods after two tectonic earthquakes with magnitudes M_L of 6.4 on the Richter scale. The two earthquakes caused different degrees of cracking at the same earth dam turn. From the results of this study, the following five conclusions are drawn:

1) Earthquakes that can induce cracks in dams are tectonic earthquakes. The primary effect of tectonic earthquakes is shear banding, while the secondary effect is ground vibrations. Therefore, seismic design codes for earth dams should not focus on only ground vibration effects.

2) After cracking occurred at the turning point of the Hutoupi Earth Dam during the 2010 Jiaxian earthquake, scholars and technicians used a conventional approach based on a ground-induced cracking mechanism for the design of the restoration project. Ground-penetrating radar and in-situ excavation were used to investigate the depth and extent of the cracking during the entire restoration process. However, as this cracking mechanism cannot completely describe the depth and extent of the cracking, the restoration project suffered water leakage in 2013 and experienced more serious cracking after the 2016 Meinong earthquake.

3) After more serious cracking occurred at the Hutoupi Earth Dam turn during the 2016 Meinong earthquake, a repair project was designed according to a cracking mechanism in which the shear bands extend into earth dams. Using the shear bands identified in a GPS velocity vector distribution map, a repair project can be designed that considers both safety and economic concerns.

4) When the shear bands extend to the crest of the Hutoupi Earth Dam at the turning point, in theory, the full section should be repaired. However, as the reservoir has a minimum wa-

ter table, it was only possible to safely repair the section above the minimum water table.

5) Since August 2016, after the Meinong earthquake, the restoration of the Hutoupi Earth Dam's turn has suffered several tectonic earthquakes with Richter magnitudes M_L ranging from 5.0 to 6.7, which shows the effectiveness of the repair. Presently, the Hutoupi Earth Dam still has no cracks at the turn. This result demonstrates that when considering the extension of shear bands into the earth dam, and the use of GC, which resists shear banding and has a low permeability, along with a comprehensive compacted soil quality management approach, the performance design goal of prevention of crack formation during tectonic earthquakes was achieved.

Based on the five conclusions presented in this study, the following two suggestions are provided:

1) The current seismic design code for dams only focuses on the effects of ground vibrations; however, ground vibration effects are not the main effects of tectonic earthquakes, and technicians carry out seismic design based on this code. Therefore, it is strongly recommended that the shear banding effect be included in the seismic design code as soon as possible.

2) When the crack extension depth and range considered in the design of the earth dam restoration project are insufficient, or when the shear banding resistance of the repair material is low, the rolling operation during repair will increase the degree of brittle fracture from the shear bands or textures in the adjacent earth dam, resulting in more serious cracking in the repaired earth dam during subsequent tectonic earthquakes. Therefore, it is suggest that this study be used as a blueprint in the future to establish a code for seismic design and construction management of earth dam restoration engineering that considers the shear banding and the ground vibration effects of tectonic earthquakes.

References

China Earthquake Disaster Prevention Center, “What happened to earthquakes: types of earthquakes,” China Digital Science and Technology Museum: Talking about the Earthquake, Website: http://amuseum.cdstm.cn/AMuseum/earthquak/1/2j-1-2.html, 2012.

Coffey, J., “What are the Different

Types of Earthquakes?" Universe Today, Space and astronomy news, Website: https://www.universetoday.com/82164/types-of-earthquakes/, 2021.

Geotechnical Engineering Manual, *GEM-12, Guidelines for Embankment Construction*, *GEM-12*, *Revision #4*, Website: https://www.dot.ny.gov/divisions/engineering/technical-services/technical-services-repository/GEM-12b.pdf, 2015.

Google Earth, Website: http://www.google.com.tw/intl/zh-TW/earth/, 2021.

GPS LAB, Website: http://gps.earth.sinica.edu.tw/, 2007.

Hsu, Tse-Shan, *Capturing Localizations in Geotechnical Failures*, Ph.D. Dissertation, Civil Engineering in the school of Advanced Studies of Illinois Institute of Technology, 1987.

Hsu, Tse-Shan, *The Major Cause of Earthquake Disasters: Shear Banding,* Institute of Mitigation for Earthquake Shear Banding Disaster, 2018.

Hsu, Tse-Shan, Hsieh, Yi-Lang and Lai, Shih-Yin, "The Professional Disaster Cause of the Houfeng Bridge: Shear Band," *Journal of Civil and Hydraulic Engineering*, Vol. 36, No. 4, pp. 1-9, 2009.

Hsu, Tse-Shan and Saxena, S. K., "A General Formula for Determining Density of Compacted Soils with Oversize Particles," *Journal of Soils and Foundations,* Vol. 31, No. 3, 1991.

Jianan Farmland Water Conservancy Association, *The General Report of the Fourth Safety Assessment of Hutoupi Reservoir*, 2012.

Lin, Zeng-Long, *Brief Report on Safety Review of Xinshan Reservoir*, Water Conservancy Construction Inspection and Safety Assessment Team's Water Storage and Diversion Working Group's second safety review in 2009, District 1 Management Office of Taiwan Water Supply Company, 2009.

Natural Resources Conservation Service Construction Specification, *North Dakota Earthfill (Code 108)*, website：ND-CS-108.pdf, 2021.

Rice, J. R., "The Localization of Plastic Deformation," in Theoretical

and Applied Mechanics (*Proceedings of the 14th International Congress on Theoretical and Applied Mechanic*s, Delft, 1976, ed. W.T. Koiter), NorthHolland, Amsterdam, Vol. 1, pp. 207-220, 1976.

Rudnicki, J. W. and Rice, J. R., "Conditions for the localization of deformation in pressure-sensitive dilatants materials," *Journal of the Mechanics and Physics of Solids*, Vol. 23, pp. 371-394, 1975.

Sinotech Foundation for Research and Development of Engineering Sciences and Technologies, "Summary of the Gouhou Dam Accident in Qinghai Province China – the case album of the dam accident", 2008.

Stephens, Tim, *Manual on Small Earth Dams: A Guide to Siting, Design and Construction*, David Lubin Memorial Library, Website: https://agris.fao.org/agris-search/search.do?recordID=XF2006443567, 2010.

Terzaghi, K. and Peck, R. B., *Soil Mechanics in Engineering practice,* 2nd ed., John Wiley & Sons, Inc., pp. 169-173, 1967.

US Army Corps of Engineers, *General Design and Construction Considerations for Earth and Rock-Fill Dams*, *Engineering and Design*, EM 1110-2-2300, Website: https://www.publications.usace.army.mil/portals/76/publications/engineermanuals/em_1110-2-2300.pdf, 2004.

US Department of the Interior, Bureau of Reclamation, *Design Standards No. 13 Embankment Dams*, Chapter 2: Embankment Design Phase 4, Website: https://www.academia.edu/23062266/Design_Standards_No_13_Embank-ment_Dams_Chapter_1_General_Design_Standards_Phase_4_Final, 2012.

Valanis, K. C., "Banding and stability in plastic materials," *Acta Mechanica*, Vol. 79, pp. 113-141, 1989.

Wagner, A. A., "The Use of the Unified Soil Classification System by the Bureau of Reclamation," *Proceedings of 4th International Conference of Soil Mechanics and Foundation Engineering*, London, Vol. 1, p. 125, 1957.

Water Resources Agency, MOEA, "Brief report on safety review of the first water storage and diversion structure of Hutoupi Reservoir in 2000," Southern District Water Resources Bureau, 2010

Water Resources Agency, MOEA, "Water Conservancy Construction Inspection and Safety Assessment Methods", 2003.

Water Resources Agency, MOEA, "Water Conservancy Construction Inspection and Safety Assessment Technical Specification", 2008.

Wendy Fisher, "Earth dam failure by internal erosion (piping)," Website: https://www.researchgate.net/figure/Earth-dam-failure-by-internal-erosion-piping-3_fig1_297714057, 2021.